Peer-reviewed version available at *Molecules* **2016**, *21*, 1498; doi:10.3390/molecules21111498

Large scale screening of Southern African plant extracts for the green synthesis of gold nanoparticles using microtitre-plate method

Abdulrahman M. Elbagory[1], Christopher N. Cupido[2,3], Mervin Meyer[1] and Ahmed A. Hussein[4*]

[1]*DST/Mintek Nanotechnology Innovation Center, Department of Biotechnology, University of the Western Cape, Private Bag X17, Bellville, 7530, South Africa.*
[2]*South African National Biodiversity Institute, Compton Herbarium, Private bag X7, Claremont 7735, South Africa.*
[3]*Department of Biodiversity and Conservation Biology, University of the Western Cape, Private Bag X17, Bellville, 7535, South Africa.*
[4]*Department of Chemistry, University of the Western Cape, Private Bag X17, Bellville, 7530, South Africa.*
**Corresponding author's e-mail: ahmohammed@uwc.ac.za*

Abstract

The preparation of gold nanoparticles (AuNPs) involves a variety of chemical and physical methods. These methods use toxic and environmentally harmful chemicals. Consequently, the synthesis of AuNPs using green chemistry has been under investigation to develop eco-friendly nanoparticles. One method to achieve this is the use of plant-derived phytochemicals capable of reducing gold ions to produce AuNPs. The aim of this study was to implement a facile microtitre-plate method to screen a large number of aqueous plant extracts to determine the optimum concentration (OC) to bio-synthesize the AuNPs. Several AuNPs of different sizes and shapes were successfully synthesized and characterized from seventeen South African plants. The characterization was done using Ultra Violet-Visible Spectroscopy, Dynamic Light Scattering, High Resolution Transmission Electron Microscopy and Energy-Dispersive X-ray Spectroscopy. We also studied the effects of temperature on the synthesis of the nanoparticles and measured its effect on the particle size of the synthesized AuNPs and the data showed that changes in temperatures affect the size and dispersity of the generated AuNPs. Further, some of the synthesized AuNPs were stable upon incubation with different biological solutions *in vitro*.

Keywords

Green nanotechnology; gold nanoparticles; biosynthesis; high resolution transmission electron microscopy; Cape flora.

Peer-reviewed version available at *Molecules* **2016**, *21*, 1498; doi:10.3390/molecules21111498

1. Introduction

Metallic nanoparticles have potential applications in chemistry, physics and biology due to their unequalled optical, electrical and photothermal properties [1]. These metal nanoparticles have drawn attention because of the ease of their synthesis and modification [2]. Among the metal nanoparticles, gold nanoparticles (AuNPs) have received much attention for their unique and adjustable Surface Plasmon Resonance (SPR) [3]. AuNPs have been utilized in several biomedical applications such as drug delivery, disease diagnosis and treatment of cancer, photothermal therapy, and immunochromatographic identification of pathogens in clinical specimens [4].

In general, the preparation of metal nanoparticles involves a variety of chemical and physical methods, such as chemical reduction [5], photochemical reduction [6], electrochemical reduction [7], laser ablation [8] and lithography [9]. These methods are expensive and involve the use of several toxic, environmentally harmful inorganic chemicals, such as sodium/potassium borohydrate, hydrazine and salts of tartrate, or organic chemicals, such as sodium citrate, ascorbic acid and amino acids, which are used for their reducing capabilities [10]. The employment of these harmful chemicals can limit the use of nanoparticles in biomedical applications [11].

Consequently, the green synthesis of AuNPs has been under investigation owing to the rising need to develop biocompatible, less-toxic and eco-friendly nanoparticles. One method to achieve this is the utilization of biological systems such as bacteria, fungi and plant extracts. For example, Kalishwaralal and co-workers synthesized gold nanocubes, ranging from 10 to 100 nm, from the bacterium *Bacillus licheniformis* after incubation with the gold salt for 48 hr [12]. Shankar *et al*., synthesized spherical AuNPs from an endophytic fungus (*Colletotrichum* sp.) after 96 hrs of incubation [13]. Several studies reported the synthesis of AuNPs using extracts from plants such as, *Aloe vera* [14], *Magnolia kobus*, *Diospyros kaki* [15], *Suaeda monoica* [16], *Trianthema decandra* [1] and *Memecylon umbellatum* [17]. These systems are not only eco-friendly, but also cost-effective and can be easily modified for large–scale synthesis [1].

The use of plants is more attractive, compared to the other biological systems, as they are readily available, safer and contain wide variety of reducing phytochemicals. Further, the plant-derived phytochemicals require shorter incubation time with the gold salt to synthesize AuNPs compared to microbial-derived chemicals [2]. These phytochemicals are not only responsible for the synthesis of metal nanoparticles, but also they act as capping agents to prevent the coalescence of colloidal particles, which are kept apart in solution by electrostatic forces [10]. It is thought that different-shaped polyol and water-soluble heterocyclic components of plant phytochemicals are mainly responsible for the reduction and coating the gold ions [17].

Peer-reviewed version available at *Molecules* **2016**, *21*, 1498; doi:10.3390/molecules21111498

The flora of the South Western Cape, which is commonly referred to as the Cape Flora or the Core Cape Sub-region of the Greater Cape Floristic Region, is the smallest and richest region in plant diversity in the world. It has over 9 300 species occupying a land area of approximately 90 000 km^2 with about 70% of the species occurring nowhere else in the world [18]. In this study, we synthesized AuNPs using seventeen plant extracts collected from the South Western Cape area of South Africa.

Herein we report the synthesis of different plant generated AuNPs. The synthesis process was monitored under two different temperature conditions to measure the effect of temperature on the geometric properties of the synthesized AuNPs. The stability of the AuNPs was measured after incubating them with different biological solutions. Several physical and optical measurement techniques such as, Ultraviolet-Visible Spectroscopy (UV-Vis), Dynamic Light Scattering (DLS), High Resolution Transmission Electron Microscopy (HR-TEM) and Energy-dispersive x-ray spectroscopy (EDS) were used to in order to characterize the nanoparticles.

2. Results and discussion

Previous studies reported the green synthesis of the plant-mediated AuNPs by mixing specific concentrations of gold salt solutions with the plant extracts solutions [1, 14, 15, 16, 17]. In this study, we sought to improve the current used methods to biosynthesize AuNPs from plants by developing micro-scale method to screen large number of plants at once. Using this method we can also determine the optimum concentrations (OC) at which the plants can reduce gold salts to AuNPs.

2.1 Preparation of AuNPs (UV-Vis analysis)

The formation of the AuNPs was first visually observed by the development of red/wine-red colour in the 96 well plates. The measurement of the UV-Vis spectra also confirmed the formation of the AuNPs. A maxima absorbance between 500 and 600 nm (Table 1), is attributed to the excitation of their surface plasmon resonance [19] and considered as a distinct feature for the presence of AuNPs. Three plant extracts, namely *A. rubicundus*, *A. hispida* and *E. rhinocertis*, did not exhibit any colour change when tested at 25 ˚C. This may indicate the absence of strong reducing phytochemicals in their aqueous extracts which needed the presence of higher temperature to initiate the reduction process. However, since in this study the extracts were incubated with the gold salt for 1 hr, these plant extracts might need a longer period to start reducing the gold ions at low temperature. Epigallocatechin gallate (EGCG), which was previously reported by Nune *et al*. to reduce gold salt [20], was used as a control to monitor the synthesize AuNPs. The λ_{max} of EGCG was 532 nm, which is within the same range of 535 nm the λ_{max} reported by Nune *et al*.

The SPR of the AuNPs is highly sensitive to many factors such as particles shape and size, the refractive index of the dispersion medium and the average distance between neighbouring AuNPs [21]. From the UV-Vis spectra of the AuNPs shown in Figure 1, it is evident that no major shifts were observed between

AuNPs synthesized at 25 ˚C or at 70 ˚C. The notable difference seen in the UV-Vis spectra for the AuNPs produced from the plant extracts was a change in the height of the peaks (which may relate to the number of the nanoparticles produced, as the OD-value correlates linearly with the concentration of the AuNPs in a solution [22]). Further, the bands generated by AuNPs synthesized at 70 ˚C were generally sharper and more symmetrical (which can be an indication of the increased uniformity in size distribution of AuNPs [23]). It is also observed that the plasmon bands of most of AuNPs are broad with an absorption tail in the longer wavelength attributing the excitation of the in-plane SPR and indicates significant anisotropy in the shape of gold nanoparticle [24] or the formation of aggregated spherical nanostructures [25]. On the other hand, green tea and EGCG (at both temperatures) showed minimum absorption tail towards the near infrared region, which may indicate their stability and/or the lack of anisotropic nanoparticles. Table 1 summarize the maxima absorbance data recorded from all the tested plants.

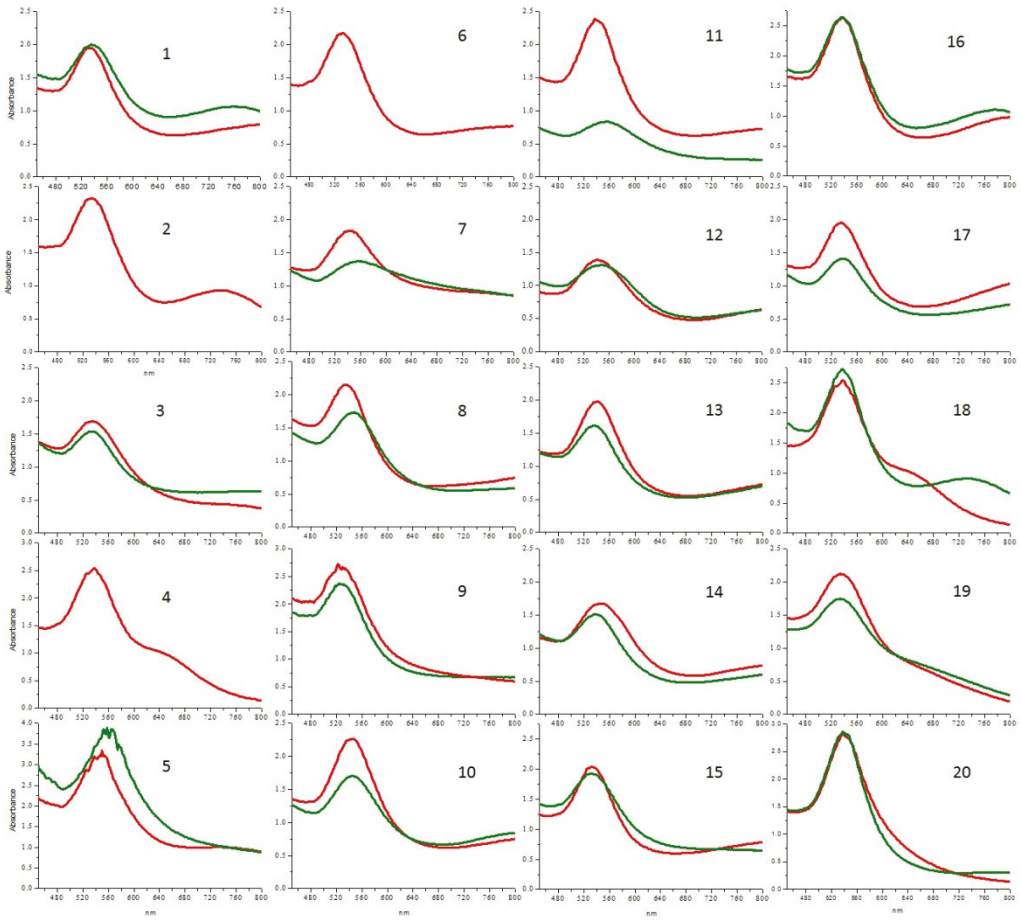

Figure 1: Comparison of the UV-Vis spectra for the AuNPs produced at 25 ˚C (green) and at 70 ˚C (red). [Numbers on each spectrum correspond to the numbers in table 1. EGCG (20) and *Camellia sinensis* (18 and 19; black and green tea) were included for comparison purpose].

Table 1: The optimum concentration (OC), particle diameter (PD), λ_{max} and average zeta potential values (ZP) of the AuNPs synthesized from the tested plants at 25 ˚C and 70 ˚C.

Plant name	25 ˚C					70˚C				
	OC (mg/mL)	λ_{max} (nm)	PD (nm)	Pdi	ZP (mV)	OC (mg/mL)	λ_{max} (nm)	PD (nm)	Pdi	ZP (mV)
1- *Anisodontea scabrosa*	1	536	78	0.398	-21	0.5	536	66	0.42	-27
2- *Aspalathus hispida*	*	*	*	*	*	0.5	534	34	0.564	-13
3- *Aspalathus linearis*	0.5	536	99	0.343	-23	0.5	536	61	0.315	-20
4- *Asparagus rubicundus*	*	*	*	*	*	1	538	28	0.66	-22
5- *Cynanchum africanum*	2	558	110	0.396	-14	0.5	546	99	0.407	-21
6- *Elytropappus rhinocertis*	*	*	*	*	*	0.5	534	63	0.551	-41
7- *Eriocephalus africanus*	1	554	67	0.565	-23	0.5	542	102	0.326	-23
8- *Indigofera brachystachya*	1	548	87	0.371	-16	1	534	100	0.477	-41
9- *Lobostemon hispidus*	0.5	552	218	0.76	-23	0.5	540	136	0.217	-26
10- *Metalasia muricata*	1	546	65	0.469	-16	0.25	544	61	0.352	-14
11- *Nidorella foetida*	0.5	564	124	0.231	-24	0.5	548	97	0.243	-28
12- *Otholobium bracteolatum*	4	546	47	0.525	-20	1	542	53	0.423	-25
13- *Podocarpus falcatus*	1	538	141	0.6	-15	0.5	540	102	0.577	-15
14- *Podocarpus latifolius*	2	540	76	0.46	-16	1	540	54	0.513	-18
15- *Salvia africana-lutea*	1	534	148	0.466	-25	0.5	534	69	0.202	-23
16- *Searsia dissecta*	0.5	538	62	0.405	-12	0.5	538	68	0.299	-14
17- *Senecio pubigerus*	1	538	75	0.519	-18	0.5	536	49	0.469	-15
18- *Camellia sinensis* (Black tea)	2	538	63	0.535	-0.2	1	540	23	0.67	-19
19- *Camellia sinensis* (Green tea)	1	535	104	0.61	-12	1	534	47	0.376	-12
20- EGCG	0.125	532	45	0.324	-26	0.125	534	52	0.311	-22

* No nanoparticles were synthesized at this condition.

Peer-reviewed version available at Molecules 2016, 21, 1498; doi:10.3390/molecules21111498

2.2 Particle size diameter, distribution and shape analysis

2.2.1 DLS analysis

Most of the plant extracts produced nanoparticles of smaller sizes at 70 ˚C (Table 1). This is in agreement with previous studies, as it was proved that lower temperatures yield larger AuNPs [26]. Pandey and co-workers reported the effect of higher temperature in optimizing the green synthesis of AuNPs and showed that smaller nanoparticles can be synthesized by increasing the temperature [27, 28]. However, in case of *I. brachystachya*, *E. africanus* and *A. scabrosa*, the AuNPs produced at 25 ˚C were smaller than those synthesized at elevated temperature. This may due to the destruction of the capping agents in those plant extracts which allow the growth of AuNPs to larger particles. Smallest AuNPs produced at 25 ˚C was generated by *O. Bracteolatum* (47 nm), while smallest AuNPs produced at 70 ˚C was obtained from green tea (23 nm) *L. hispidus* gave the largest AuNPs diameters of 218 nm and 136 nm at 25 ˚C and 70 ˚C, respectively.

The polydispersity index (Pdi) values in table 1 also shows that the AuNPs are often more monodispersed when synthesized at 70 ˚C. The Pdi represents the ratio of particles of different size to total number of particles, so the lower the value of Pdi the more monodispersed are the particles. Arockiya Aarthi Rajathi and co-workers reported the synthesis of AuNPs from the leaves of *Suaeda monoica* with a Pdi value of 0.286, which was considered to be a representation of monodispersed particles [16]. AuNPs from *N. foetida* gave the lowest Pdi values both at 25 ˚C and 70 ˚C.

2.2.2 HRTEM and EDX analysis

The TEM images of the AuNPs, produced from plant extracts (figure 2), showed variable geometrical shapes and sizes. However, AuNPs produced from some extracts showed a dominance of some shapes over others. The presence of the anisotropic particles in the samples is indicated by the presence of absorbance towards the near infra red region in their spectra. On the other hand, EGCG AuNPs were mostly uniform in shape and such uniformity was reflected with minimum absorbance towards the near infra red region. Overall, larger particles from ~ 150 nm in size were mostly triangular, truncated triangular, and hexagonal in shape. On the other hand, smaller nanoparticles were mostly, spherical, pentagonal and hexagonal, although few small triangles could also be observed. This mixture of geometrical shapes is a common feature of AuNPs as reported before [29, 30]. TEM images show only a few particles in each frame, hence statistically reliable distributions of these shapes and sizes cannot be evaluated using TEM [31]. Moreover, there were no apparent difference in the shapes between AuNPs synthesized at 25˚C and 70˚C as seen for AuNPs synthesized from *P. latifolius*. One interesting observation from the TEM images is the presence of a halo surrounding most of the nanoparticles (Figure 3). This halo was also observed by Zeiri *et al*., which has a width of 2 to 3 nm, and was suggested to protect the AuNPs from aggregation [31].

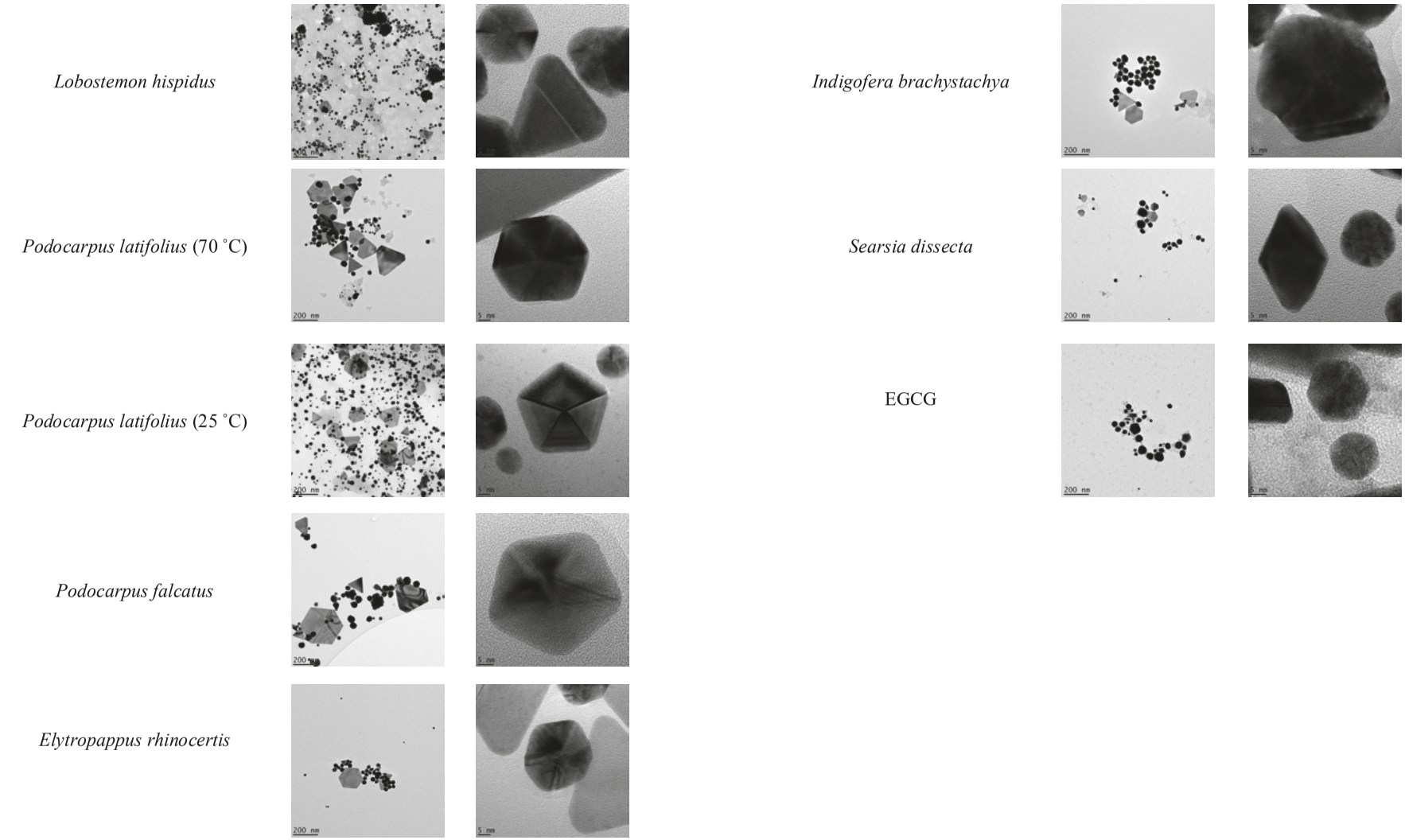

Figure 2: TEM images of the synthesized AuNPs.

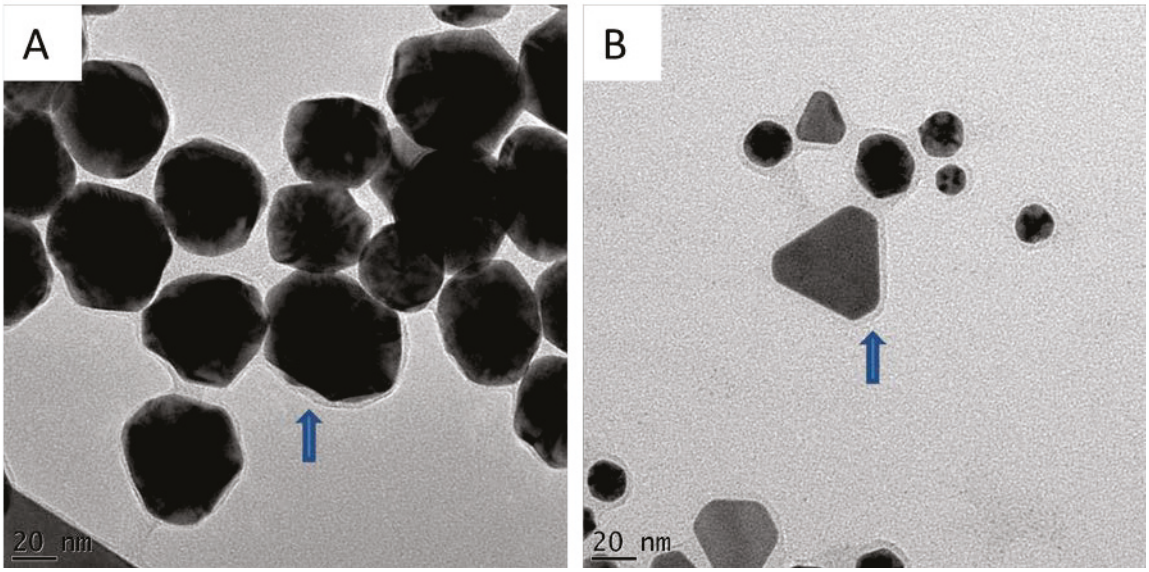

Figure 3: TEM images of AuNPs produced from a) *I. brachystachya* and b) *A. rubicundus* showing a halo surrounding the nanoparticles

The EDX spectroscopy analysis of the AuNPs confirmed the presence of gold ions in the samples selected for TEM analysis. Strong optical adsorption peaks were observed at around 2.3, 9.7 and 11.3 KeV, which are consistent with a previous study (Figure 4) [17]. The presence of strong peaks of carbon and copper, and silicon in some samples, is attributed to the TEM grid and the detector window [32], whereas the presence of calcium, oxygen, potassium and chloride is suggested to be traces from the phytochemicals of the extracts and the gold salt [16, 31].

Lobostemon hispidus

Podocarpus latifolius

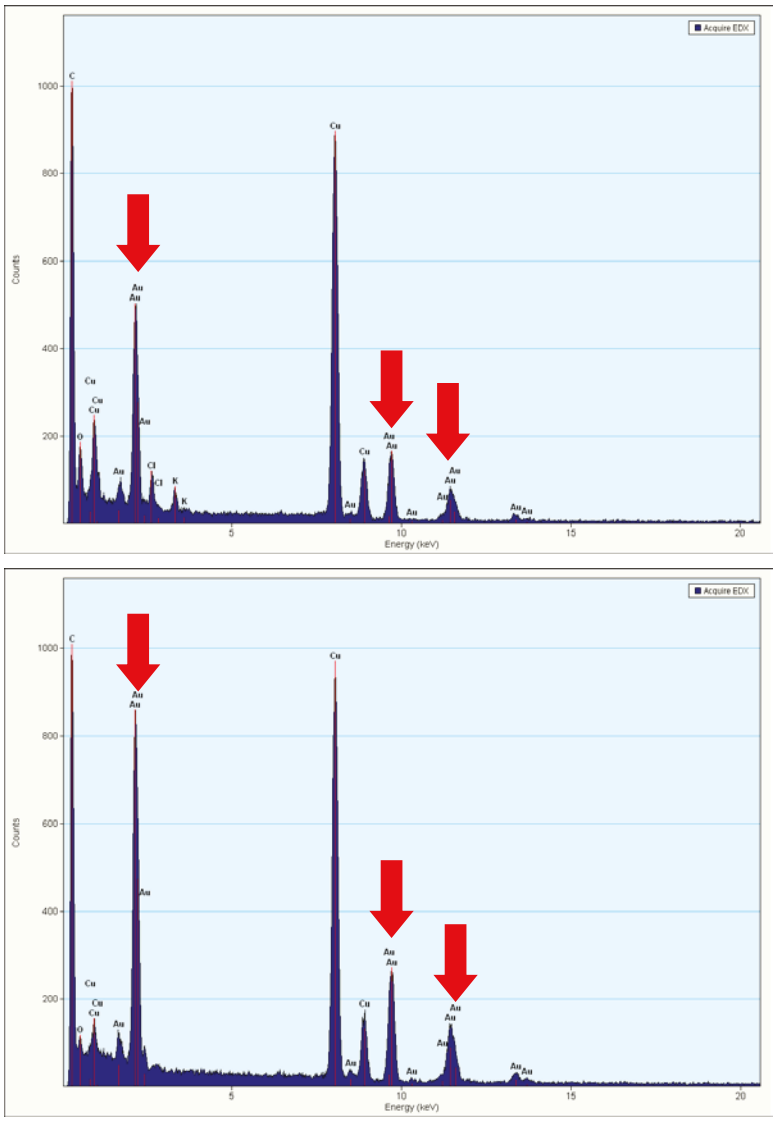

Figure 4: EDX spectra of some AuNPs showing Au peaks in red arrows.

Peer-reviewed version available at Molecules 2016, 21, 1498; doi:10.3390/molecules21111498

3.2 Stability of the AuNPs

The zeta potential values of the synthesized AuNPs were measured in order to evaluate their stability. All measurements of the samples were done immediately upon synthesis. Generally, the zeta potential can be used to anticipate the long term stability of AuNPs in a solution, as the magnitude of the charge reflects the mutual repulsion forces between the particles [33]. All of the plant extracts demonstrated negative zeta potential as shown in table 2. Overall, a negative zeta potential value is suggested that the particles will be stable in solutions [33].

To further evaluate the stability of the AuNPs, they were incubated for extended periods under different biological solutions. Biologically stable AuNPs should not aggregate (manifested by minimal changes in the UV-Vis spectra) under a wide range of environmental conditions (e.g: salts and biological additives) [33]. In this study, the AuNPs were incubated with 10% NaCl, 0.5% cysteine and 0.5% Bovine Serum Albumin (BSA). The stability of AuNPs was monitored by recording their UV-Vis spectra over different time intervals. Only AuNPs synthesized from *P. latifolius* and *A. rubicundus* showed excellent stability by retaining their surface plasmon resonance (Figure 5). This indicates that these nanoparticles are highly stable at different environmental conditions and hence can be used in different medical applications and assays. On the other hand, none of the other AuNPs synthesized from the other plant extracts showed a similar stability upon incubation with the same biological solutions. For instance, the AuNPs generated from *O. bracteolatum* and *A. linearis* did not exhibit the same minimal changes in their respective UV-Vis specta shown in figure 6. It is suggested that the flattening in their SPR is contributed to the formation of larger particles over the time of incubation, where also the decrease of their intensities may be contributed to the reduction of the AuNPs in terms of their number especially when incubated with 0.5% BSA.

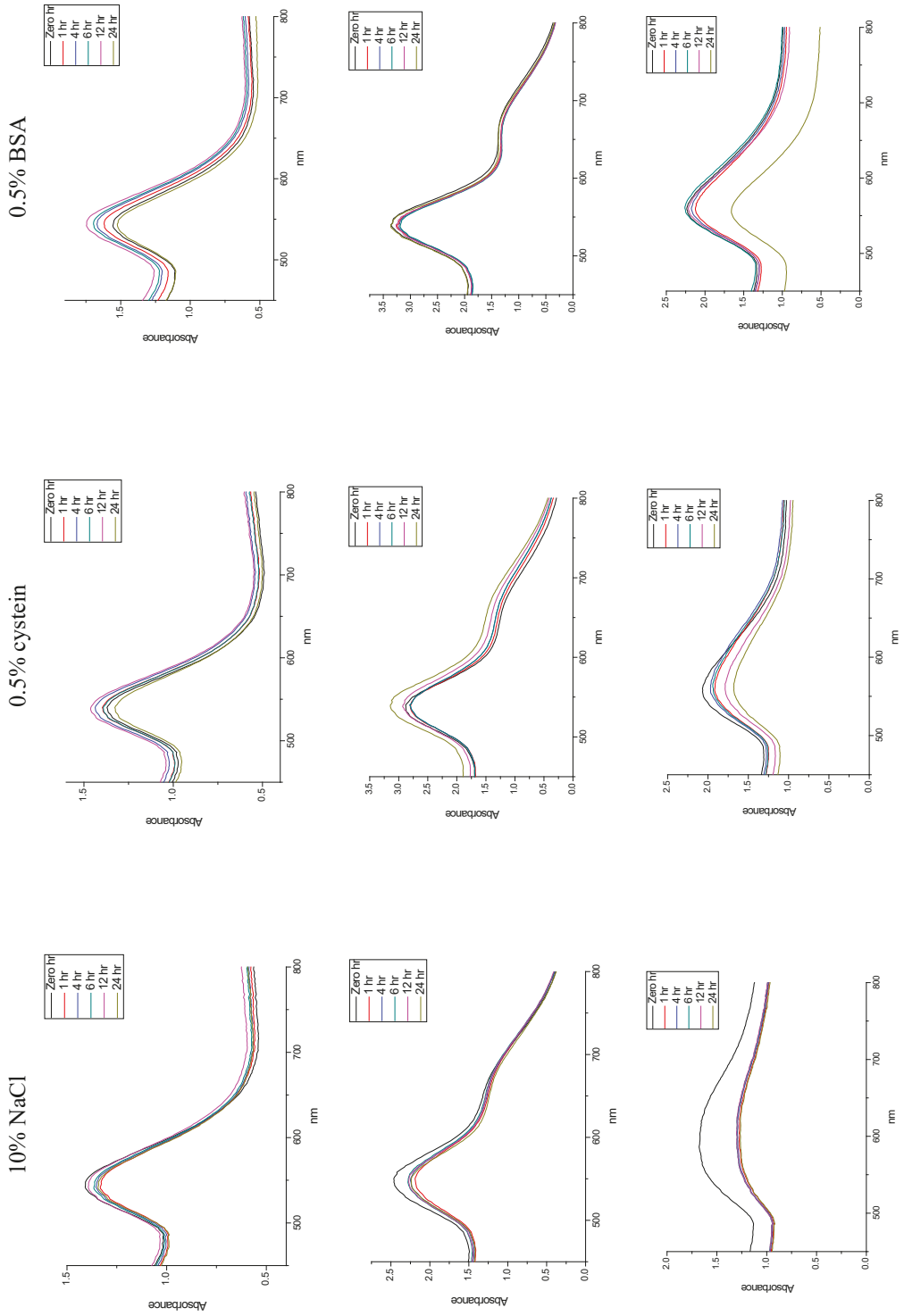

Podocarpus latifolius

Asparagus rubicundus

Otholobium bracteolatum

Aspalathus linearis

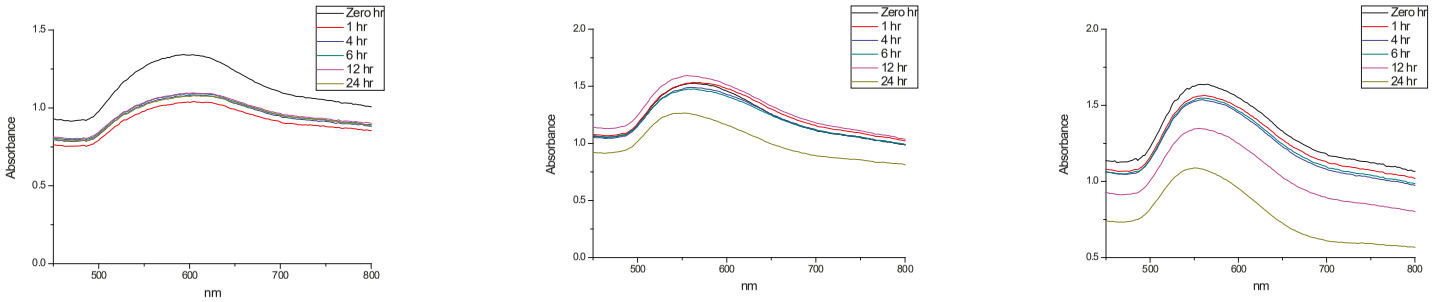

Figure 5: Changes in UV-Vis spectra of AuNPs over 24 hr period in buffers containing 10% NaCl, 0.5% cysteine and 0.5% BSA.

Preprints (www.preprints.org) | NOT PEER-REVIEWED | Posted: 11 August 2016 doi:10.20944/preprints201608.0120.v1

Peer-reviewed version available at Molecules 2016, 21, 1498; doi:10.3390/molecules21111498

3.3 Effect of temperature on AuNPs characteristics

In order to view the effect of elevated temperature on the overall synthesis of the AuNPs, the average values of the particle diameter, λ_{max}, and Pdi values were calculated (Table 2). It was previously reported that high temperatures can produce AuNPs of better size distribution [28]. The measurement of the particle size distribution of some AuNPs supported that report. For example, in figure 6 it can be observed that at elevated temperature the AuNPs synthesized from *E. africanus* exhibited better size distribution in contrast to the AuNPs synthesized at lower temperature. Overall, the higher temperature the smaller and better defined the particles were, which is also correlated with the blue shift of the λ_{max}. This is in agreement with the study conducted by Mountrichas and co-workers [28]. Song et al. explained the formation of smaller AuNPs at high reaction temperature by stating that most gold ions are consumed in the formation of the nuclei with the increase of reaction temperature as a result of increased reaction rate, therefore preventing the secondary reduction process of the performed nuclei and hence stopping the formation of larger AuNPs [34].

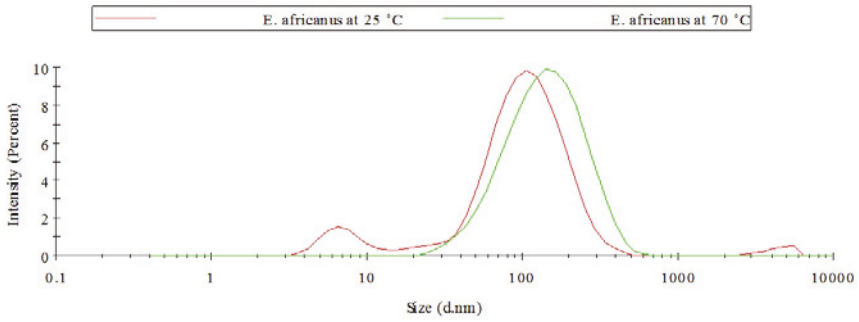

Figure 6: Particle size distribution for AuNPs produced from *E. africanus.*

Table 2: The average particle diameter, λ_{max}, and Pdi values obtained from all the plant extracts at 25 ˚C and 70 ˚C.

	25 ˚C	**70 ˚C**
λ_{max} (nm)	543 ± 9	539 ± 4
particle diameter (nm)	97 ± 44	68 ± 29
Pdi	0.465± 0.127	0.419 ± 0.14

3.4 Effect of concentration and determination of OC for each plant extract.

The optimum concentration is simply defined as the concentration at which a plant extract produce smaller and uniform NPs. To investigate the effect of plant extract concentration; fixed concentration of gold salt was incubated with different concentrations of the plant extracts (16 – 0.007 mg/ml). We based our selections of the OC first on the SPR (λ_{max}) and the uniformity of the Uv-Vis curve, and second on the PD and Pdi values which give an indication of the uniformity of the AuNPs produced. Thereafter, for further analysis, the chosen concentrations (OC) were used to synthesize the AuNPs after scaling up the volumes

Preprints (www.preprints.org) | NOT PEER-REVIEWED | Posted: 11 August 2016 doi:10.20944/preprints201608.0120.v1

Peer-reviewed version available at Molecules 2016, 21, 1498; doi:10.3390/molecules21111498

along with the adjacent concentrations in the first screening step. It was observed that higher temperature yielded smaller particle sizes at lower concentrations of the plant extracts. Figure 7 shows that the optimum concentration at 25˚C is 1 mg/mL, while at 70˚C it is 0.5 mg/mL. No uniform and small AuNPs were synthesized at concentrations higher than 4 mg/mL.

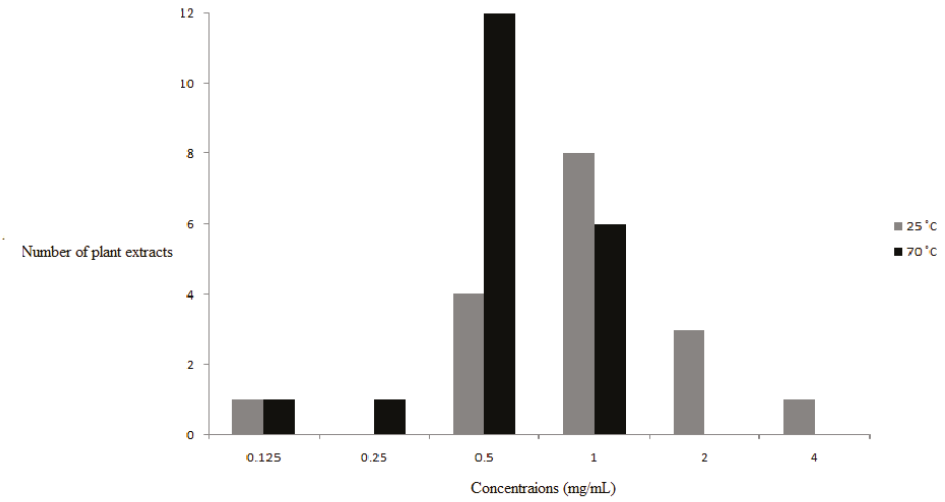

Figure 7: Optimum concentrations for AuNPs synthesis for all plant extracts at 25 ˚C and 70 ˚C.

In figure 8, we selected, as an example, the SPR of one of the tested controls (EGCG) and a plant extract (*P. latifolius*) to show the growth pattern of the AuNPs under different concentrations. At low concentrations both of the SPR exhibited red shifts, this indicates the formation of AuNPs of large particle size (EGCG at 0.0625 mg/mL gave λ_{max} at 550 nm with particles of average diameter of 393 nm, at 1 mg/mL *P. latifolius* had λ_{max} of 554 nm with average diameter of 79 nm). By increasing the concentration of the reducing material (EGCG or the plant extracts) smaller particle diameter were obtained and the OCs were reached. The SPR of the OCs exhibited the maximum blue shift compared to the SPR of the lower concentrations. At this point, the growth pattern comes with agreement the nucleation-growth mechanism of the citrate AuNPs proposed by Frens [35]. Frens showed that smaller citrate AuNPs can be obtained by increasing the sodium citrate (reducing agent) concentration while using fixed gold salt concentration. It was suggested that the citrate AuNPs were grown through a fast nucleation process followed by controlled diffusion growth at which average sizes can be reduced as sodium citrate concentrations increased. However, as we increase the concentration of the reducing material beyond the OC (0.125 mg/mL for EGCG and 2 mg/mL for *P. latifolius*) no smaller AuNPs were obtained as expected, on the contrary the SPR curves became more flat and/or red shifted as the concentrations increase, which is a clear indication of the increased average size of the AuNPs as discussed in section 2.1. For instance, EGCG gave AuNPs of

Peer-reviewed version available at Molecules 2016, 21, 1498; doi:10.3390/molecules21111498

particle diameter of 55 nm and λ_{max} of 536 nm at 0.25 mg/mL compared to 45 nm and 532 nm at 0.125 mg/mL. In the case of *P. latifolius* no shifts were observed compared to the optimum concentration curve, but instead the SPR curves became more flat and showed absorbance above 600 nm, which are indications of the formation of larger particles (particle diameter of 83 nm at 4 mg/mL and 207 nm at 16 mg/mL).

Ji and co-workers [36], observed that citrate AuNPs were produced with larger diameter by increasing the sodium citrate above certain limit. It was proved that AuNPs can be produced under two different pathways that yield different sizes. These pathways were determined based on the pH of the medium. They proved that above a certain critical pH value the AuNPs grow differently via Ostwald ripening which leads to the formation of larger AuNPs. In their study, the pH of the reaction mixture was dependent on the initial sodium citrate/gold salt ratio. In another study, Guo and co-workers [37] also reported the effect of changing the pH on the synthesis of AuNPs from *Eucommia ulmoides* bark aqueous extract. They proved that at pH values above certain optimum value the reaction mixture turned blue with no absorption peak due to the formation of larger and aggregated AuNPs. This was also observed in this study with EGCG at 8 mg/mL (see inset figure 8 A). While the *P. latifolius* mixture at highest concentration tested (16 mg/ mL) started to give bluish red colour compared to the rosy red colour of the OC (see inset figure 8 B). We presume a similar mechanism occurs in our study, because, the change in pH is slightly small between the small and high concentrations, we are proposing other factor(s) as well that cause non-linearity relationship between the plant extract concentration and the formation of NPs. We assume that, at high concentration above the OC the crowded media causes a certain degree of impedance that prevent the reducing and/or capping agents to function well. The plant extract generally containing unlimited number of phytochemicals, some of them at high concentration may insulate or reverse the action of the reducing and/or capping agents. Therefore, the determination of OC where the interaction of the plant extract with gold salt reach the optimum, highly appreciated and considered to be the best concentration ratio for the synthesis of NPs, above the OC the growth pattern of the NPs change and produce larger particle.

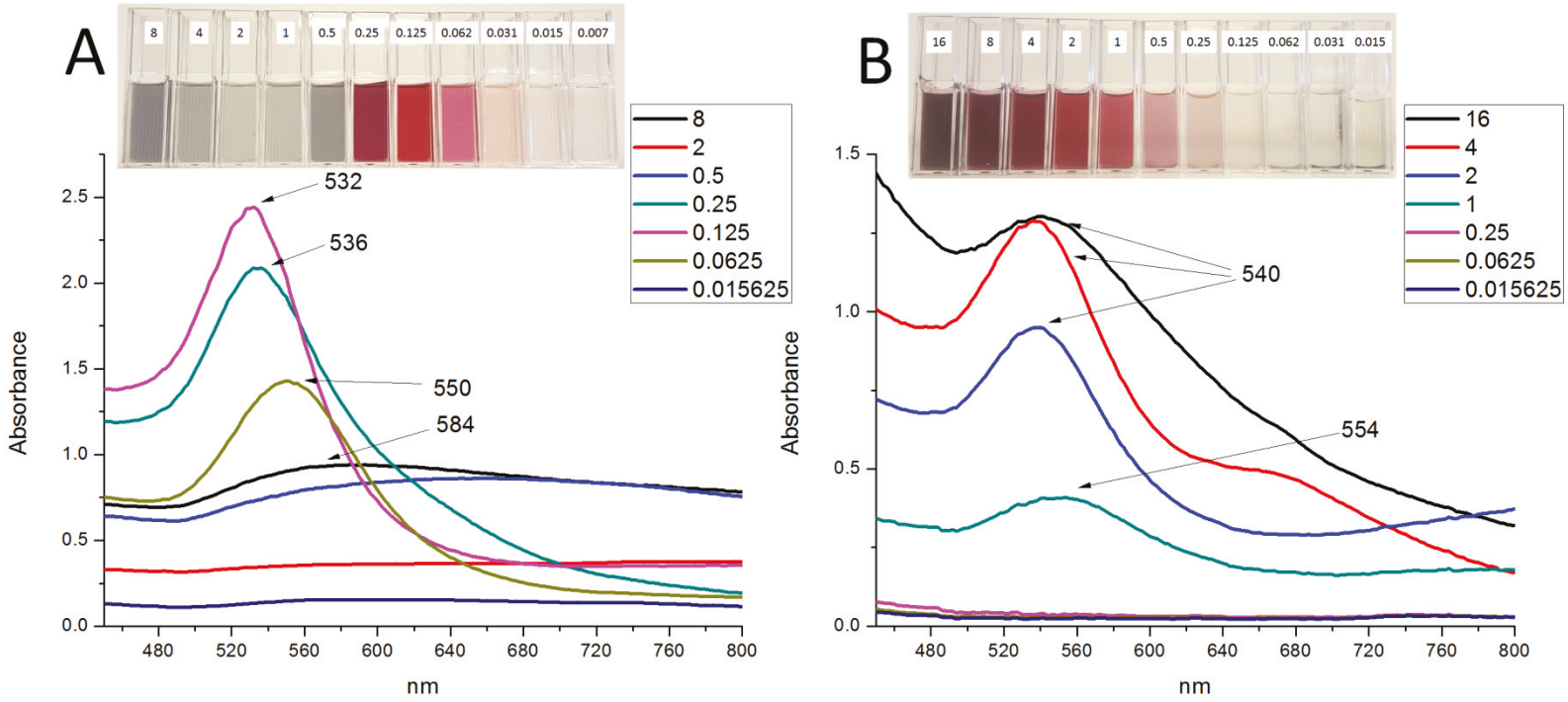

Figure 8: UV-Vis spectra for the AuNPs produced from A) EGCG and B) *P. latifolius* using different concentrations (mg/mL) at 25 ˚C.

4 Materials and Methodology

4.1 Materials

C. sinensis (black and green tea) and *A. linearis* (Rooibos tea) were purchased from local vendors in South Africa, EGCG from Zhejiang Yixin Pharmaceutical Co., Ltd (China), 96 well polystyrene microplates from Greiner bio-one GmbH (Germany), gold salt (sodium tetrachloroaurate (III) dehydrate) from Sigma-Aldrich (USA), Bovine Serum Albumin (BSA) from Miles Laboratories (USA), N-Acetyl-L-cystein from Boehringer Mannheim GmbH (Germany) and sodium chloride (NaCl) from Merck (USA).

4.2 Instruments

Centrifugation for the extracts was done using Allegra® X-12R (Beckman Coulter, USA). The AuNPs were centrifuged using Centrifuge 5417R (Eppendorf AG, Germany). The extracts were freeze dried using FreeZone 2.5L (Labconco, USA). UV-Vis spectra were recorded using POLARstar Omega microplate reader (BMG Labtech, Germany). The particle size, size distribution and zeta potential measurements of the freshly synthesized AuNPs in solution were analyzed using Zeta sizer (Malvern Instruments Ltd., USA). TEM analysis was done using FEI Tecnai G^2 20 field-emission gun (FEG).

4.3 Sample collection

Plant samples (Table 3) were collected during May 2015 from two sites in the Western Cape Province of South Africa. The first site is situated in Malmesbury (GPS coordinates: 33°27'33.44"S, 18°44'39.87"E) approximately 60 km north of the University of the Western Cape. The vegetation on this site is classified as the critically endangered Swartland Granite Renosterveld. In contrast, the second site is situated approximated 20 km south of the university in Mfuleni (GPS coordinates: 34°00'18.54"S, 18°41'8.19"E) and supports an endangered vegetation unit known as Cape Flats Dune Strandveld. On both sites the sampling strategy was random and all the specimens collected were identified and deposited at the Compton Herbarium (NBG), Kirstenbosch, Cape Town, South Africa. The collection and identification process was performed by C.N. Cupido the co-author of this paper.

Preprints (www.preprints.org) | NOT PEER-REVIEWED | Posted: 11 August 2016 doi:10.20944/preprints201608.0120.v1

Peer-reviewed version available at Molecules 2016, 21, 1498; doi:10.3390/molecules21111498

Table 3: The collected plants and their herbarium number.

Plant name	Herbarium number
Anisodontea scabrosa	AB-1-20
Aspalathus hispida	AB-1-4
Asparagus rubicundus	AB-1-1
Cynanchum africanum	AB-1-6
Elytropappus rhinocertis	AB-1-11
Eriocephalus africanus	AB-1-13
Indigofera brachystachya	AB-1-16
Lobostemon hispidus	AB-1-17
Metalasia muricata	AB-1-9
Nidorella foetida	AB-1-12
Otholobium bracteolatum	AB-1-25
Podocarpus falcatus	*
Podocarpus latifolius	*
Salvia africana-lutea	AH-42
Searsia dissecta	AB-1-21
Senecio pubigerus	AB-1-14

* *P. falcatus* and *P. latifolius* were purchased from Kristenboch national botanical garden, Cape Town, South Africa.

4.4 Preparation of the plant extracts

Fresh plant materials were dried in the shade for two weeks, grinded and extracted using boiled distilled water using the following ratio: 50 mL of distilled water to 5 g of plant material. The plant decoctions were centrifuged at 3750 rpm for 2 hrs. The supernatants were then freeze dried. A stock solution of 32 mg/mL was freshly prepared for each extract before the experiment.

4.5 Screening of gold nanoparticles synthesis

The gold salt concentration was fixed at 1 mM [17] and incubated with increasing concentrations of the plant extracts (16 to 0.007 mg/mL). 50 µl of plant extracts were added to 250 µl of gold salt (ratio 1:5). The plates were incubated at 25˚C and 70˚C with shaking (40 rpm) for 1 hr. The SPR of the AuNPs was measured by recording the UV-Vis spectrum from range 300 nm to 800 nm. For further characterization and stability evaluations, the synthesis of the AuNPs from the tested plants was scaled up using the concentrations of the plant extracts that produced AuNPs.

4.6 High resolution transmission electron microscopy (HRTEM) and energy dispersive X-ray spectroscopy (EDX) analysis

To study the surface morphology of the AuNPs, samples were prepared by drop-coating one drop of each sample solution onto a holey carbon coated copper grid. This was then dried under a Xenon lamp for 10 min, where after the sample coated grids were analyzed under the microscope. Transmission electron

Peer-reviewed version available at *Molecules* **2016**, *21*, 1498; doi:10.3390/molecules21111498

micrographs were operated in bright field mode at an accelerating voltage of 200 kV. Energy dispersive x-ray spectra were collected using an EDAX liquid nitrogen cooled Lithium doped Silicon detector.

4.7 Stability evaluation of the synthesized AuNPs

In vitro stability of the synthesized AuNPs was measured by incubating the AuNPs with different aqueous solutions of NaCl, cystein and BSA. First, the synthesized AuNPs were centrifuged at 10,000 rpm for 5 min. The pellets were washed three times with distilled water to remove phytochemicals that are not capping the gold nanoparticles. The nanoparticles were re-suspended in 1 mL autoclaved distilled water. Thereafter, 100 µL of the tested AuNPs solutions was incubated with equal volume of the biological media in 96 well plate. The final concentrations of the biological media in the final mixture was as follows; 10% NaCl, 0.5% cystein and 0.5% BSA [33]. The stability of the AuNPs was evaluated by measuring the changes in UV-Vis spectra after 1, 4, 6, 12 and 24 hrs.

5 Conclusion

This study was designed to investigate the effect of the concentration of different plant extracts on the formation of AuNPs on microscale. The results showed nonlinear relationship between concentrations and the formed AuNPs, and we determined a specific concentration (for each plant extract) called OC at which a smaller and uniform AuNPs were obtained.

The aqueous extracts of the tested plants were used to reduce Au^{+3} to Au^{0} and form the AuNPs. *C. sinensis* (black and green tea) as well as EGCG were used as controlling agents for the AuNPs synthesis screening process. This study shows for the first time a fast and easy screening method of a large number of aqueous plant extracts for the bio-synthesis of AuNPs. The formation of AuNPs by this approach has several advantages since it reduces cost and time of the synthesis in addition of being environmental-friendly. The synthesized AuNPs were thoroughly studied, and their shapes, size and *in vitro* stability were examined. Of total seventeen plants collected for this study, all of them produced AuNPs at two different temperatures (25 ˚C and 70 ˚C), except for *A. rubicundus*, *A. hispida* and *E. Rhinocertis,* which only produced AuNPs at 70 ˚C. The formation of the AuNPs was confirmed by the presence of their characteristic SPR in the UV-Vis spectra.

We also applied different reaction conditions and showed that smaller particle size and more defined AuNPs can be achieved by applying high temperature during the synthesis process. The particle sizes were studied by DLS analysis, which also gave indication about the AuNPs stability in aqueous solutions. Of all plant extracts, green tea produced the smallest AuNPs with an average diameter of 23 nm at 70 ˚C. TEM analysis showed the geometrical shapes of the AuNPs, and was with agreement to the UV-Vis. EGCG was able to synthesize AuNPs of uniform shapes according to the TEM analysis, which was also reflected in its UV-Vis results. The EDX analysis also confirmed the presence of gold ions in the samples by recording noticeable optical adsorption peaks of gold ions at the same ranges that were reported before in the literature. By monitoring the stability of the SPR bands of the synthesized AuNPs, under different

environmental conditions, we were able to determine three plants extracts namely *P. latifolius* and *A. rubicundus*. To expand on this, we suggest studying the toxicity of these stable AuNPs against human cell lines to determine their potential in further biomedical applications.

Acknowledgment

A.M. Elbagory would like to thank the DST/Mintek Nanotechnology Innovation Centre (NIC) and the National Research Foundation (NRF) for funding his PhD study.

Author Contributions

A.M. Elbagory, M. Meyer and A.H. Hussein conceived and designed the experiments and analyzed the data; C.N. Cupido collected and identified the plants; A.M. Elbagory performed the experiments and drafted the paper; A.H. Hussein coordinated writing the paper to which all co-authors contributed.

Conflicts of Interest

The authors declare no conflict of interest.

References

1- Geethalakshmi, R.; Sarada, DVL. Gold and silver nanoparticles from Trianthema decandra: synthesis, characterization, and antimicrobial properties. *Int. J. Nanomedicine*. **2012**, 5375. doi:10.2147/ijn.s36516.

2- Nath, D.; Banerjee, P. Green nanotechnology – A new hope for medical biology. *Environ. Toxicol. Phar*. **2013**, 36, 997-1014. doi:10.1016/j.etap.2013.09.002.

3- El-Sayed, M. Some interesting properties of metals confined in time and nanometer space of different shapes. *Acc. Chem. Res*. **2001**, 34, 257-264. doi:10.1021/ar960016n.

4- Huang, X.; El-Sayed, I.; Qian, W.; El-Sayed, M. Cancer cell imaging and photothermal therapy in the near-infrared region by using gold nanorods. *J. Am. Chem. Soc*. **2006**, 128, 2115-2120. doi:10.1021/ja057254a.

5- Yu, D. Formation of colloidal silver nanoparticles stabilized by Na+–poly(γ-glutamic acid)–silver nitrate complex via chemical reduction process. *Colloids Surf. B*. **2007**, 59, 171-178. doi:10.1016/j.colsurfb.2007.05.007.

6- Mallick, K.; Witcomb, M.; Scurrell, M. Self-assembly of silver nanoparticles in a polymer solvent: formation of a nanochain through nanoscale soldering. *Mater. Chem. Phys.* **2005**, 90, 221-224. doi:10.1016/j.matchemphys.2004.10.030.

7- Liu, Y.; Lin, L. New pathway for the synthesis of ultrafine silver nanoparticles from bulk silver substrates in aqueous solutions by sonoelectrochemical methods. *Electrochem. Commun.* **2004**, 6, 1163-1168. doi:10.1016/j.elecom.2004.09.010.

8- Tsuji, T.; Kakita, T.; Tsuji, M. Preparation of nano-size particles of silver with femtosecond laser ablation in water. *Appl. Surf. Sci*. **2003**, 206, 314-320. doi:10.1016/s0169-4332(02)01230-8.

9- Jensen, T.; Malinsky, M.; Haynes, C.; Van Duyne, R. Nanosphere lithography: tunable localized surface plasmon resonance spectra of silver nanoparticles. *J. Phys. Chem. B.* **2000**, 104, 10549-10556. doi:10.1021/jp002435e.

10- Lukman, A.; Gong, B.; Marjo, C.; Roessner, U.; Harris, A. Facile synthesis, stabilization, and anti-bacterial performance of discrete Ag nanoparticles using *Medicago sativa* seed exudates. *J. Colloid Interface Sci.* **2011**, 353, 433-444. doi:10.1016/j.jcis.2010.09.088.

11- Shankar, S.; Rai, A.; Ahmad, A.; Sastry, M. Rapid synthesis of Au, Ag, and bimetallic Au core–Ag shell nanoparticles using Neem (*Azadirachta indica*) leaf broth. *J. Colloid Interface Sci.* **2004**, 275, 496-502. doi:10.1016/j.jcis.2004.03.003.

12- Kalishwaralal, K.; Deepak, V.; Ram Kumar Pandian, S.; Gurunathan, S. Biological synthesis of gold nanocubes from *Bacillus licheniformis*. *Bioresour. Technol*. **2009**, 100, 5356-5358. doi:10.1016/j.biortech.2009.05.051.

13- Shankar, S.; Ahmad, A.; Pasricha, R.; Sastry, M. Bioreduction of chloroaurate ions by geranium leaves and its endophytic fungus yields gold nanoparticles of different shapes. *J. Mater. Chem.* **2003**, 13, 1822. doi:10.1039/b303808b.

14- Kumar, V.; Yadav, S. Plant-mediated synthesis of silver and gold nanoparticles and their applications. *J. Chem. Technol. Biotechnol*. **2009**, 84, 151-157. doi:10.1002/jctb.2023.

15- Song, J.; Jang, H.; Kim, B. Biological synthesis of gold nanoparticles using *Magnolia kobus* and *Diopyros kaki* leaf extracts. *Process Biochem*. **2009**, 44, 1133-1138. doi:10.1016/j.procbio.2009.06.005.

16- Arockiya Aarthi Rajathi, F.; Arumugam, R.; Saravanan, S.; Anantharaman, P. Phytofabrication of gold nanoparticles assisted by leaves of *Suaeda monoica* and its free radical scavenging property. *J. Photochem. Photobiol. B.* **2014**, 135, 75-80. doi:10.1016/j.jphotobiol.2014.03.016.

17- Arunachalam, K.; Annamalai, S.; Shanmugasundaram, H. One-step green synthesis and characterization of leaf extract-mediated biocompatible silver and gold nanoparticles from *Memecylon umbellatum*. *Int. J. Nanomedicine*. **2013**, 8, 1307-1315. doi:10.2147/ijn.s36670.

18- Manning, J. & Goldblatt, P. Plants of the Greater Cape Floristic Region 1: the Core Cape flora, *Strelitzia* 29. **2012**, South African National Biodiversity Institute, Pretoria.

19- Rastogi, L.; Arunachalam, J. Microwave-assisted green synthesis of small gold nanoparticles using aqueous garlic (*Allium sativum*) extract: their application as antibiotic carriers. *Int. J. Green Nanotechnol*. **2012**, 4, 163-173. doi:10.1080/19430892.2012.676926.

20- Nune, S.; Chanda, N.; Shukla, R.; Katti, K.; Kulkarni, R.; Thilakavathi S.; Mekapothula S.; Kannan, R.; Katti, KV. Green nanotechnology from tea: phytochemicals in tea as building blocks for production of biocompatible gold nanoparticles. *J. Mater. Chem.* **2009**, 19, 2912-2920. doi:10.1039/b822015h.

21- Guo, L.; Jackman, J.; Yang, H.; Chen, P.; Cho, N.; Kim, D. Strategies for enhancing the sensitivity of plasmonic nanosensors. *Nano Today*. **2015**, 10, 213-239. doi:10.1016/j.nantod.2015.02.007.

22- Abdelhalim, M.; Mady, M.; Ghannam, M. Physical properties of different gold nanoparticles: ultraviolet-visible and fluorescence measurements. *J. Nanomedic. Nanotechnol*. **2012**, 3 doi:10.4172/2157-7439.1000133.

23- Saifuddin, N.; Wong, C.; Yasumira, A. Rapid biosynthesis of silver nanoparticles using culture supernatant of bacteria with microwave irradiation. *E-J. Chem*. **2009**, 6, 61-70. doi:10.1155/2009/734264.

24- Narayanan, K.; Sakthivel, N. Coriander leaf mediated biosynthesis of gold nanoparticles. *Mater. Lett*. **2008**, 62, 4588-4590. doi:10.1016/j.matlet.2008.08.044.

25- Shipway, A.; Lahav, M.; Gabai, R.; Willner, I. Investigations into the electrostatically induced aggregation of Au nanoparticles. *Langmuir*. **2000**, 16, 8789-8795. doi:10.1021/la000316k.

26- Zhu, J.; Kónya, Z.; Puntes, V.; Kiricsi, I.; Miao CX.; Ager J.; Alivisatos A.; Somorjai G. Encapsulation of metal (Au, Ag, Pt) nanoparticles into the mesoporous SBA-15 structure. *Langmuir*. **2003**, 19, 4396-4401. doi:10.1021/la0207421.

27- Pandey, S.; Oza, G.; Mewada, A.; Sharon, M. Green synthesis of highly stable gold nanoparticles using *Momordica charantia* as nano fabricator. *Arch. Appl. Sci. Res.* **2012**, 4, 1135-1141

28- Mountrichas, G.; Pispas, S.; Kamitsos, E. Effect of temperature on the direct synthesis of gold nanoparticles mediated by polydimethylaminoethyl methacrylate homopolymer. *J. Phys. Chem. C.* **2014**, 118, 22754-22759. doi:10.1021/jp505725v.

29- Chen, R.; Wu, J.; Li, H.; Cheng, G.; Lu, Z.; Che, C. Fabrication of gold nanoparticles with different morphologies in HEPES buffer. *Rare Metals*. **2010**, 29, 180-186. doi:10.1007/s12598-010-0031-5.

30- Foss, C.; Hornyak, G.; Stockert, J.; Martin, C. Template-synthesized nanoscopic gold particles: optical spectra and the effects of particle size and shape. *J. Phys. Chem.* **1994**, 98, 2963-2971. doi:10.1021/j100062a037.

31- Zeiri, Y.; Elia, P.; Zach, R.; Hazan, S.; Kolusheva, S.; Porat, Z. Green synthesis of gold nanoparticles using plant extracts as reducing agents. *Int. J. Nanomedicine.* **2014**, 9, 4007-4021. doi:10.2147/ijn.s57343.

32- Rodríguez-León, E.; Iñiguez-Palomares, R.; Navarro, R.; Herrera-Urbina, R.; Tánori, J.; Iñiguez-Palomares, C. Maldonado A. Synthesis of silver nanoparticles using reducing agents obtained

from natural sources (*Rumex hymenosepalus* extracts). *Nanoscale Res. Lett.* **2013**, 8, 318. doi:10.1186/1556-276x-8-318.

33- Chanda, N.; Shukla, R.; Zambre, A.; Mekapothula, S.; Kulkarni, R.; Katti, K.; Bhattacharyya, K.; Fent, G.; Casteel, S.; Boote, E.; Viator, J.; Upendran, A.; Kannan, R.; Katti, KV. An effective strategy for the synthesis of biocompatible gold nanoparticles using cinnamon phytochemicals for phantom CT imaging and photoacoustic detection of cancerous cells. *Pharm. Res*. **2010**, 28, 279-291. doi:10.1007/s11095-010-0276-6.

34- Song, J.; Jang, H.; Kim, B. Biological synthesis of gold nanoparticles using *Magnolia kobus* and *Diopyros kaki* leaf extracts. *Process Biochem*. **2009**, 44, 1133-1138. doi:10.1016/j.procbio.2009.06.005.

35- Frens, G. Controlled nucleation for the regulation of the particle size in monodisperse gold suspensions. *Nat. Phys. Sci*. **1973**, 241, 20-22. doi:10.1038/physci241020a0.

36- Ji, X.; Song, X.; Li, J.; Bai, Y.; Yang, W.; Peng, X. Size control of gold nanocrystals in citrate reduction: the third role of citrate. *J. Am. Chem. Soc*. **2007**, 129, 13939-13948. doi:10.1021/ja074447k.

37- Guo, M.; Li, W,; Yang, F.; Liu, H. Controllable biosynthesis of gold nanoparticles from a *Eucommia ulmoides* bark aqueous extract. *Spectrochim. Acta Mol. Biomol. Spectrosc.* **2015**, 142, 73-79. doi:10.1016/j.saa.2015.01.109.